NOTICE
This report was prepared as an account of work sponsored by the United States Government. Neither the United States nor the United States Energy Research and Development Administration, nor any of their employees, nor any of their contractors, subcontractors, or their employees, makes any warranty, express or implied, or assumes any legal liability or responsibility for the accuracy, completeness or usefulness of any information, apparatus, product or process disclosed, or represents that its use would not infringe privately owned rights.

MASTER

By acceptance of this article, the publisher or recipient acknowledges the U.S. Government's right to retain a nonexclusive, royalty-free license in and to any copyright covering the article.

PHYSICS AND ENGINEERING ASPECTS OF THE EBT REACTOR*

N. A. Uckan, E. S. Bettis, C. L. Hedrick, R. T. Santoro, H. L. Watts, and H. T. Yeh
Oak Ridge National Laboratory
Oak Ridge, Tennessee 37830

CONF-771029--81

Summary

The ELMO Bumpy Torus (EBT) reactor has the advantages of high-β, steady-state operation. The first reactor study based on the EBT confinement concept was initiated in 1976. It provided the required starting point for continued assessment of the validity of the concept. Recent refinements in plasma engineering and plasma physics have resulted in a revised system description. Reactor design and engineering studies have been revised and improved continually to incorporate increased understanding from the plasma research. A new design based on the present physics understanding, practical design approaches, and present and near-term technologies has been established. One of the important factors in an EBT reactor is that the large aspect ratio (large toroidal major radius as well). This leads to a power plant with a comparatively large total energy output, usually in the range of 2000-6000 MW(th) for a conventional neutron wall loading of 1-2 MW/m^2 (the high value of β in an EBT device provides a net cost per unit energy roughly equal to or somewhat less than that for a tokamak system). The large aspect ratio also provides very simple engineering and design requirements because of good access and small force loading asymmetries. Another important factor is the steady-state operation. In an EBT system, less power handling, energy storage, and filtering equipment will be needed. An EBT reactor is less likely to be subject to thermal and mechanical fatigue than reactors with large pulsed magnetic fields and short bursts of fusion power. The details of the key design elements and critical scientific and technology factors which are substantially different from other fusion reactor approaches are described.

Introduction

The experimental results from EBT[1] have motivated a consideration of the EBT concept as the basis for a potential reactor.[2,3] Since the first round of conceptual EBT reactor design in 1976,[2] there has been considerable progress in design improvement which incorporates the increased understanding from the plasma research.[3]

A power-producing EBT Reactor (EBTR) system is especially attractive from the viewpoint of a reactor designer because of its steady-state operation at high plasma pressure, its modular construction, its relatively large aspect ratio, and its favorable geometry for ease of maintenance.

The following set of design parameters is specified in order to select the reference design: from the utilities point of view, power output is limited to 2000-6000 MW(th); neutron wall loading is in the range of 1-2 MW/m^2 from wall lifetime considerations; the mirror ratio required for annulus formation is typically 2:1;[1] the limiting plasma pressure is in the range of 25-50%;[4] and the device should be capable of ignition and should use, if possible, 150-keV Tokamak Fusion Test Reactor (TFTR) neutral beams or 120-GHz EBT-II microwave sources for the toroidal plasma and 70-GHz EBT-II microwave sources for the sustaining of annuli. On the basis of trade-off studies among the plasma physics requirements and uncertainties, engineering design, and technological capabilities, a self-consistent set of plasma parameters and a range of machine characteristics, given in Table I, are obtained. In view of the uncertainties involved in each area, plausible estimates have been made to retain flexibility so the system can accommodate changes as the physics and technology evolve with time. The essential features of the EBTR are described below. This design is based on a presently acceptable plasma model[5] and relatively conservative engineering parameters.

Table I

EBT Reactor Parameters

Plasma radius (m)	1.0
Mirror ratio	1.8
Magnetic field (midplane/mirror) (T)	2.5/4.5
Aspect ratio	30-60
Number of sectors	24-48
Particle density (m^{-3})	1.4×10^{20}
Ion/electron temperature (keV)	15
Toroidal plasma β (%)	27
Neutron wall loading (average) (MW/m^2)	1.47
Total fusion power [MW(e)]	1000-2000
Cold zone (m)	0.2
Blanket thickness (m)	0.6
Shield thickness (m)	0.55
Coil inner radius (m)	3.0
Coil outer radius (m)	3.7
Coil half axial length (m)	1.05
Current density (A/cm^2)	1525
Neutral beam energy (keV)	150[a]
Neutral beam power (MW)	50-200[a]
Microwave frequency (GHz)	
Toroidal plasma	120[a]
Hot electron annuli	70
Microwave power (MW)	
Toroidal plasma	50-200[a]
Hot electron annuli	5-10

[a]A toroidal plasma will be heated to ignition conditions using either microwaves or neutral beam injection. Power required for ignition is in the range of 50-200 MW (total) depending on the start-up procedures.

Plasma Performance

The basic EBT operation requires a toroidal bumpy magnetic field structure with an electron-cyclotron-heated, hot electron ring (annulus) contained in each bump of the field. These annuli produce a local magnetic well which provides stability for the toroidal plasma.[2,4] Hence an EBT contains two different groups of particles: a comparatively small number of mirror-trapped energetic electrons (several hundred kilovolts) and a higher density (both ions and electrons) toroidal plasma. The fusions occur between the toroidal plasma ions.

The power density which will dictate the desirable characteristics for the plasma in a deuterium-tritium (D-T) burning system is given by

$$\frac{P_{TH}}{V} = N_i^2 \frac{\langle\sigma v\rangle}{4} Q_F \propto \beta^2 B^4 \frac{\langle\sigma v\rangle}{T^2} , \qquad (1)$$

where Q_F = 17.6 MeV. In a low-β plasma, β is limited to a few percent [it may be as large as 5-10% in a flux-conserving tokamak[6] (FCT)], and $\langle\sigma v\rangle/T^2$ exhibits a broad maximum between 10 and 20 keV, while the magnetic

*Research sponsored by the Department of Energy under contract with Union Carbide Corporation.

DISTRIBUTION OF THIS DOCUMENT IS UNLIMITED

field is limited by the technological constraints; an optimum operating point which is consistent with the overall plant can be chosen within these criteria. In a high-β system, additional trade-offs are involved: for example, operation outside the range which maximizes $\langle\sigma v\rangle/T^2$ might become desirable to keep the density (n) within limits because of microwave cutoff or neutral beam penetration requirements. The trade-offs involved in the optimization of the high-β cycle are unique and are formulated for the study [2,3] The trade-offs between β and B have been considered and high-β and low-B (the minimum field strength assumed feasible is ~25 kG) operation is found to be desirable. Figure 1 shows the relationship between plasma, magnetic field, and power production parameters.

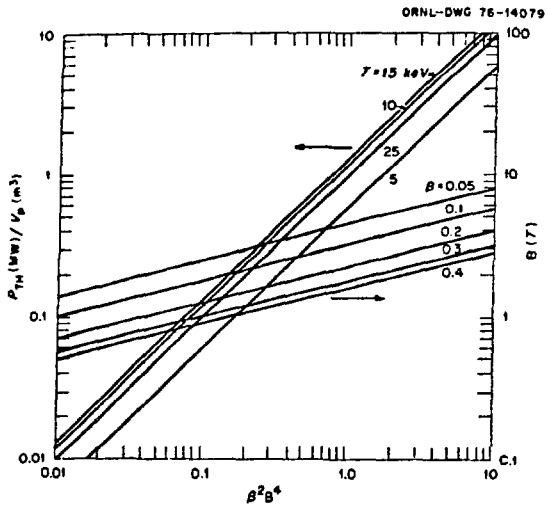

Fig. 1. Relationship between plasma, magnetic field, and power-producing parameters.

Start-up scenarios consistent with microwave cutoff (120 GHz) or neutral beam penetration (150 keV) requirements have been derived to take advantage of high-β operation in EBT. At T = 15 keV, a β of ≤0.35 is required for 120 GHz microwave penetration. Similarly, neutral beam attenuation, which is proportional to exp $(-n\sigma X)$, also places a restriction on maximum density if hollow density profiles are to be avoided. The dynamics of the EBTR system have been analyzed to establish procedures for achieving a high-β operating point at acceptable density, consistent with constraints imposed by other reactor support systems.

Steady-state plasma performance parameters are obtained from a consistent solution of the equilibrium and the plasma particle and power balance equations.[5] The scaling laws which will ultimately apply to the EBTR plasma are presently uncertain. A simulation model which retains the essential physics of the phenomena has been developed[5] to assess the plasma behavior. In this model, which is time-dependent, the toroidal plasma is characterized by simple energy and particle containment times with appropriate density and temperature scaling. The reactor plasma simulated in this model is consistent with the results obtained from EBT-I experiments:[1,5] a toroidal core with nearly uniform density and temperature within the plasma radius, which is determined by the stabilizing hot electron annuli. Early comparisons between a simple point model[7] and the experimentally observed ion and electron temperatures, plasma density, and energy confinement time for a toroidal core plasma in EBT-I indicated that the EBT-I has parameters entirely consistent with neoclassical predictions.[8] Although in the present EBT device plasma transport seems to be governed largely by neoclassical processes, hypothesized anomalous transport losses are included in the plasma simulation model in order to test the sensitivity of EBTR parameters.

From appropriate transport coefficients, confinement times are given by

$$\tau^{-1} = \gamma_{NC}\tau_{NC}^{-1} + \gamma_A\tau_A^{-1} \quad . \tag{2}$$

The γ factors permit consideration of different containment times, where the subscripts "NC" and "A" correspond to neoclassical and anomalous processes, respectively. The scaling of confinement time with density (n) and temperature (T) for neoclassical and anomalous processes is given by[5,7,8]

$$\tau_{NC} \propto \frac{3}{4}\left[\frac{R_T}{R_C}(1 + Z_j\eta)\right]^2 \left(\frac{1 + \nu_j^2/\Omega_j^2}{\nu_j}\right) \quad j = e,i, \tag{3}$$

$$\tau_A \propto \frac{n^s}{T^p} \tag{4}$$

where

$$\nu_j = 3.8 \times 10^{-17} \frac{Z_j^2 n_j}{\sqrt{A_j}\,T_j^{3/2}} \ , \tag{5}$$

$$\Omega_j = 10^3 \frac{T_j}{Z_j B R_c a}(1 + Z_j\eta) \text{ with } \eta = 10^{-3}\frac{E_r R_c}{T_j} \ . \tag{6}$$

All units are mks (temperatures and in keV).

R_T and R_c are the toroidal and minor radii of curvature, and s and p are constants. From Eq. (2) one can arrange to have

$$\left(\frac{\gamma_A}{\tau_A}\right) = \frac{T^p}{n^s}\left[\left(\frac{n^s}{T^p}\right)_o \left(\frac{\gamma_{NC}}{\tau_{NC}}\right)_o F\right] \ , \tag{7}$$

where the subscript "o" corresponds to the operating point values (steady state) and F (anomaly factor) is an adjustable constant which is chosen to yield physically plausible solutions. The results of the calculations for various values of the anomaly factor F and electric field parameter η are given in Fig. 2. It is shown (see Fig. 2) that the selected parameters for EBTR are flexible enough to accommodate anomalous losses one to two orders of magnitude greater than the present neoclassical losses at the operating point.

Fueling of the EBT reactor is required to take advantage of steady-state operation; however, this requirement is not unique since it applies to all large systems where the burn time will exceed the particle containment time. In EBT-I particle density is maintained by introducing neutral gas into the chamber. The EBTR plasma is too large (~1 m) to permit adequate neutral penetration for this technique to be effective, so the particle density will be maintained by some other means, such as pellet fueling.

A method for removing residues (fusion products) and impurities may be necessary if particle dynamics of transport processes do not lead to this result naturally. In EBT-I, impurities do not accumulate in the central region of the plasma due to the short confinement of impurities on surface plasma and shielding by the ring electric field. Either future experiments will validate EBT-I results or the EBTR will require a residue removal and impurity control mechanism.

Power requirements to sustain the stabilizing annuli need to be examined in detail, although preliminary calculations show that this is not a problem because the ring plasma occupies a relatively small volume.[2,3] In steady state, the annulus power balance is $P_{\mu A} = P_{\tau A} + P_{BA} + P_{CA}$, where $P_{\tau A}$ is thermal conduction and convection, P_{BA} is bremsstrahlung losses, P_{CA}

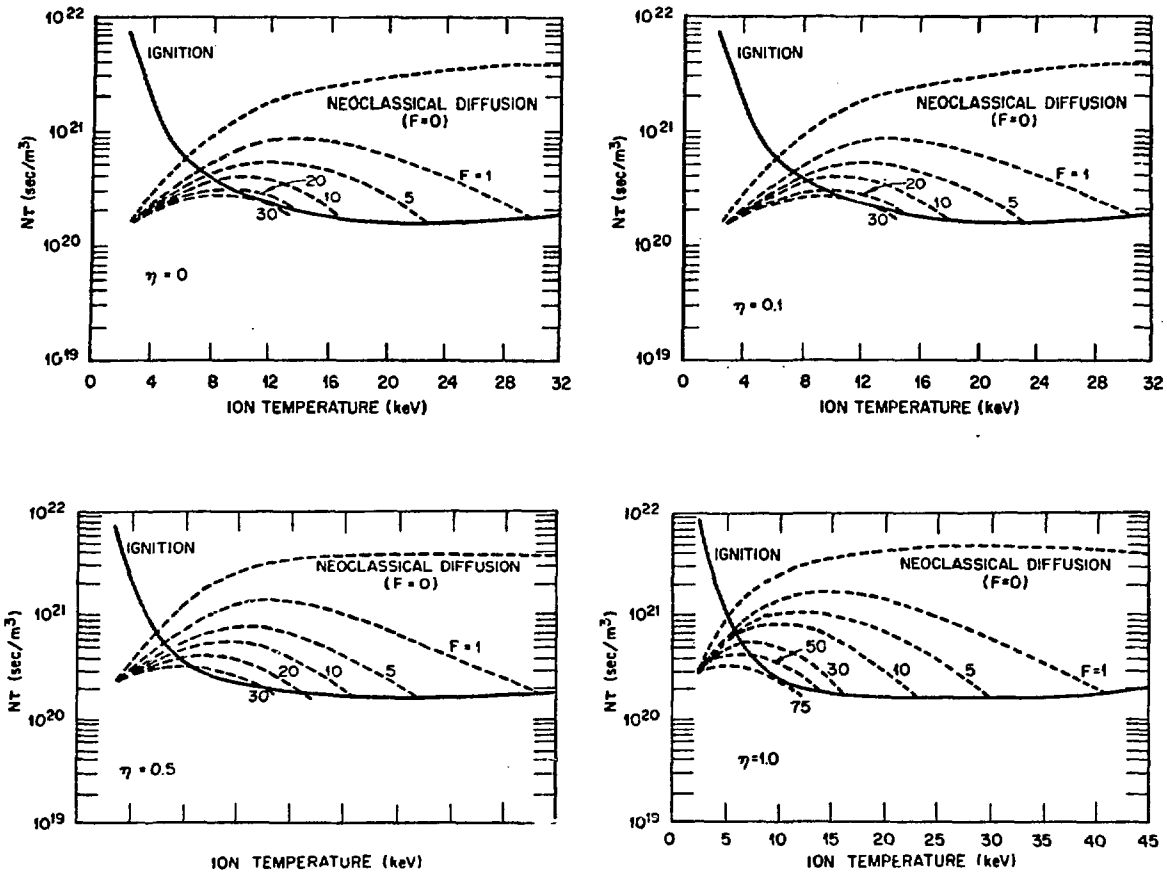

Fig. 2. Nτ vs ion temperature T_i for different values of anomaly factor F and the electric field parameter η.

is synchrotron (cyclotron) radiation, and $P_{\mu A}$ is the microwave power required to sustain the annulus. The emission of synchrotron radiation from the hot electron annulus in EBT and the large-scale EBTR was estimated in Ref. 1. More detailed calculations have been carried out for the EBTR reference design.[2] In the latter work, the synchrotron emission amounted to a few tens of kilowatts per sector at worst, compared to a few tens to a few hundreds of kilowatts of transport losses for the data chosen. It is important, however, that this subject be reviewed frequently as more information becomes available about the annuli (and their scaling laws) from the future experiments[1] (EBT-S/SA, EBT-II, ...).

A comparison of the parameters of EBT-I and those projected for EBT-S/SA, EBT-II, ..., EBTR yields an interesting result. Virtually all the dimensionless parameters which influence stability are roughly the same in EBT-I, EBT-II, and the projected EBTR. Thus, the following dimensionless parameters are either the same or in the direction of increased stability: annular beta; ratio of gyroradii to various scale lengths; field errors; aspect ratio; ratio of cold to hot electron density; ratio of electron to ion temperature; ratio of electron plasma frequency to cyclotron frequency; and ratio of ambipolar potential to temperature. The β of the toroidal core plasma and, to a lesser extent, the collisionality are factors which change appreciably. The approximate constancy of these dimensionless parameters which are known to influence stability is very encouraging, and the extrapolation of EBT-I results to EBTR appears feasible.

For a high-β, steady-state EBT system, the plasma equilibrium, particle orbits, ambipolar electric field, and transport phenomena are closely coupled to one another. From these interrelations, specifically from equilibrium requirements and efficiency of use of the magnetic field, a displaced aperture-inner wall design has been adopted this year. Figure 3 shows the mod-B contours and field lines for one sector of EBTR for the straight cylindrical wall design (original wall design from last year's study) and for the displaced aperture flux following wall design (without finite β). In the latter case, the plasma is shifted about 25 cm from the coil toward the major axis. This change leads to a usable volume of about 100%,[3] compared to about 50%[2] for the straight cylindrical case.

ORNL-DWG 77-7375

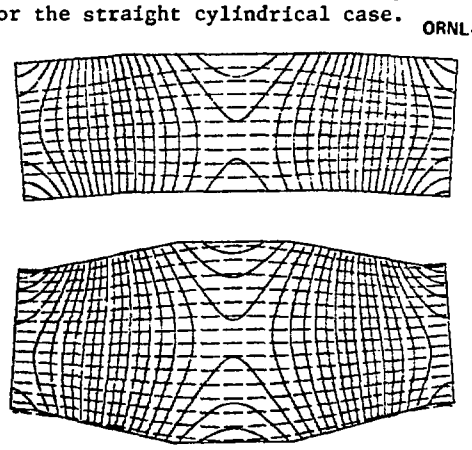

Fig. 3. Mod-B contours (solid lines) and field lines (dashed lines) in the equatorial plane for one sector of EBTR for straight cylindrical (upper curve) and displaced aperture (lower curve) inner wall design. In the upper curve, the boundary is the inner wall (and the coil planes). In the lower curve, the aperture has

been moved toward the major axis about 25 cm so that its projection along field lines into the midplane lies on mod-B contours.

Magnetics

The magnetic field in the EBTR is produced by 24 (48) 6-m-bore NbTi superconducting coils with a maximum field of about 7.8 T at the coil. The magnetic fields at the magnet throat and at the midplane (confining magnetic field) are 4.5 T and 2.5 T respectively, which gives a mirror ratio of 1.8. As long as the ratio of the reactor major radius to the number of coils is constant, the axial field strength produced is not sensitive to the size of the reactor. Thus, an important advantage of an EBTR is that the same module-magnet design can be used in reactors of different size and output. Also, EBT has a large aspect ratio, so that the magnetic field is reasonably uniform at the coils and the magnetic forces are nearly symmetrical. All coils are circular in shape and are made of tightly wound pancakes with pool-boiling cooling.

Cryostability of the magnet is achieved by building up monolithic multifilamentary NbTi composite with formed copper strips. The copper strips are punched with slots to increase the wetted surface area and to improve coolant circulation. A high operating current (25 kA) was chosen to hold the terminal voltage during discharge to 2 kV, and four conductors are wound in parallel to maintain a reasonably small conductor and large heat transfer surface. The four conductors are interleaved in a spiral fashion in such a way that inductances are equalized and the total current is evenly divided between conductors. In EBT, it is important that the field errors be small. The winding scheme adopted (see Fig. 4) gives lower field errors than if only one conductor is used. Furthermore, compensation of field errors due to the crossover currents is possible. Stray fields are further reduced by careful use of the leads as compensation for each other and for axial current component with the winding. The design provides 35% helium space, interconnected helium passages with a minimum cross-sectional dimension of 0.25 cm, and a surface heat flux of 0.15 W/cm^2 when the entire current is in the stabilizer. Quench detection is based on voltage taps, with pickup coils on the current leads of all power supplies to compensate the inductive voltages and leave only the resistive component. Eight consecutive magnets are charged with a single power supply. Each coil is individually protected by an external dump resistor, which is switched into the circuit on the detection of a quench in any coil. Details of the EBTR magnets are discussed in Refs. 2, 3, and 9.

Mechanical Design

Conceptual designs of EBT reactors based on the modular concept are studied for a wide range of sizes.[2,3] Each module consists of one superconducting magnet coil, a shield of articulated cylindrical units, and multiple blanket modules (roughly conforming to the plasma shape), as well as vacuum pumping and microwave injection ports.

The blanket is divided into segments both poloidally and toroidally. There are nine toroidal segments in one module, and each segment consists of twelve buckets arranged in a circular frame. The blanket is of uniform thickness, 60 cm, for all segments. The buckets are filled with lithium for neutron absorption and tritium production. The back section of each bucket has stainless steel spheres mixed with lithium for gamma absorption. Double wall cooling tubes are coiled in the buckets. Helium gas at 70 atm is circulated through the blanket to remove the heat for steam generation. The entire blanket structure is 316 stainless steel with a small addition of titanium. The shield sections are made of stainless steel containers (tanks) filled with stainless steel spheres around which borated water is circulated for heat removal. These tanks are divided into appropriate shapes and sizes to permit access to the blanket with relative ease.

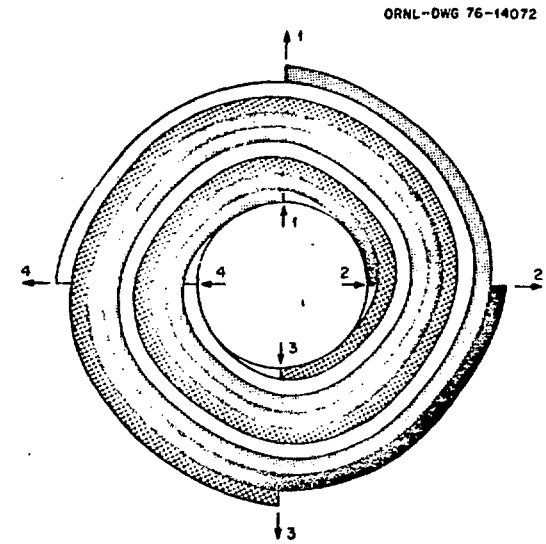

Fig. 4. Schematic diagram for spiral winding of four conductors in parallel in a pancake.

The torus is assembled in a concrete moat which is evacuated to provide a secondary vacuum enclosure for the machine. This vacuum environment greatly simplifies the assembly procedure and, more importantly, eases the remote maintenance problem, since it is not necessary to provide a vacuum-tight primary enclosure for the plasma. Thus, the individual blanket segments are not required to be welded together. Also, the numerous penetrations through the blanket need no welding to the blanket wall. All assembly and remote maintenance operations are performed from above the moat. Two gantry cranes, capable of rotating completely around the moat, are mounted on a continuous circular track. A general plan view of the entire EBTR plant is shown in Fig. 5.

The coils are installed in a concrete "picture frame." The gravity load and the magnetic centering forces are transmitted to the picture frame through laminated load-bearing pads of insulating material and a liquid-nitrogen-cooled buffer zone. A plan view of the components of the torus is shown in Fig. 6. After the coils are installed, the articulated shield pieces are installed, except for the center clamshell sections between coils. These are put in after the blanket sections have been put in place.

The plasma region is maintained at a lower pressure than the moat by two vacuum pumping ports between each toroidal field (TF) coil. Microwave injection is made through these same vacuum ports. The vacuum system for the plasma region is located in tunnels running radially under the moat. The large area encircled by the moat is used for microwave generators and power supplies, cryogenic refrigerators, primary heat exchangers, and other equipment. This central location minimizes the lengths of lines running to these auxiliaries.

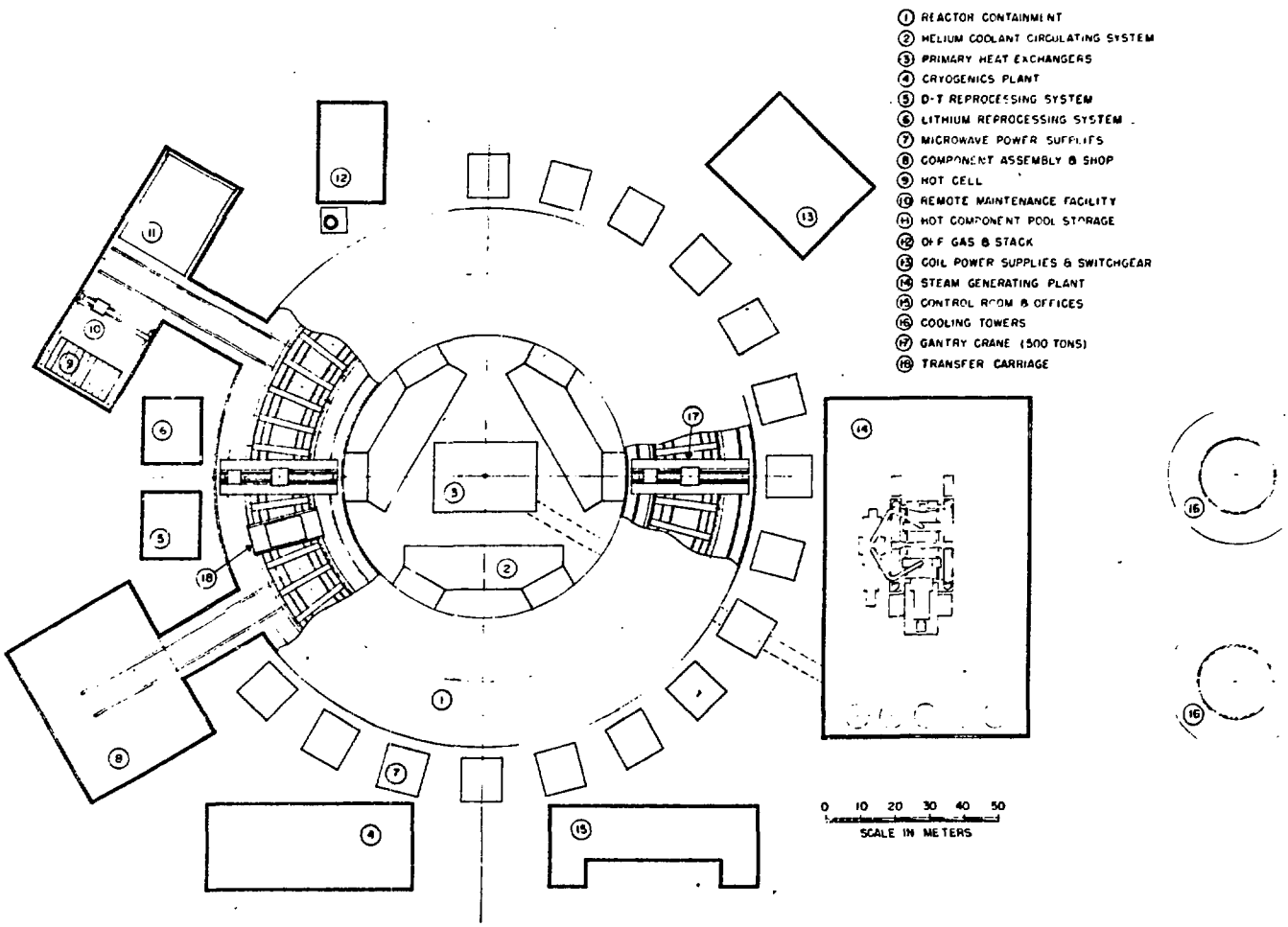

Fig. 5. EBTR plan view.

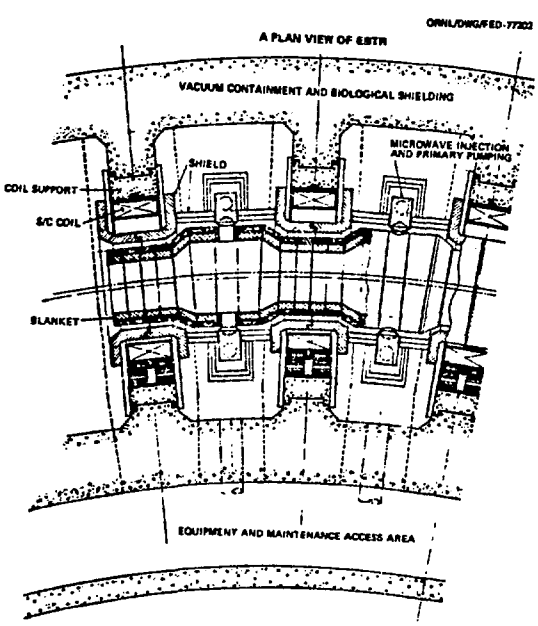

Fig. 6. A plan and section elevation view.

Neutronics Performance

Neutronics calculations were carried out to assess the ability of the lithium-laden blanket assembly to recover the kinetic energy of D-T fusion neutrons and secondary gamma rays in the form of heat and for breeding tritium. Also, the blanket and the shield assembly were evaluated in terms of their combined shielding ability to protect the magnet assembly from the intense plasma radiation.

The calculations were performed in a one-dimensional cylindrical geometry using the discrete ordinates code ANISN[10] with a P_3-S_{12} approximation. The neutron and gamma ray transport cross sections were taken from the DLC-37[11] library and collapsed to a 35-neutron and 21-gamma-ray energy group subset. All of the nuclear responses were obtained using the latest available ENDF/B-IV data. The reactor, modeled from detailed engineering drawings, has a 60-cm-thick blanket assembly consisting of lithium in a 316 stainless steel structure and cooled with high pressure helium. The blanket surrounds a 100-cm-radius plasma region with a 20-cm cold zone. The shield is 55 cm thick and is separated from the blanket by a 30-cm-thick maintenance void. The shield is composed of 316 stainless steel (65%) and water (35%) and is supported by a stainless steel structure. Surrounding the blanket and shield is a magnet assembly consisting of Nb-Ti/Cu coils and supported by stainless steel. All of the data were normalized to a first wall neutron loading of 1.47 MW/m^2.

The blanket assembly recovers 96% of the neutron and secondary gamma-ray energy in the form of heat. Approximately 4% of the energy is deposited in the

is deposited in the shield and the remainder, $(7 \times 10^{-4})\%$, is deposited in the magnet assembly. The total heating rate in the reactor is 1.47×10^5 W. The peak heating rate in the blanket is 13.5 W/cm^3 and drops off to 0.34 W/cm^3 at the front of the shield. The shield reduces the nuclear heating by nearly four orders of magnitude and at the front of the magnet assembly the peak heating is down to 5.8×10^{-5} W/cm^3.

Natural lithium is used as the fertile material in the blanket. The tritium breeding ratio is 1.29 tritium nuclei per incident neutron, with 56% of the breeding resulting from neutron reactions with ^{6}Li.

Economic Potential

In order to establish the economic potential of the EBT reactor, two independent system costing models have been developed. The first model relies on an explicit model of EBTR[2,3] to compute the cost of the reactor itself and on the United Engineers and Constructors 1972 plant cost estimate developed for the liquid metal fast breeder reactor (LMFBR) (suitably inflated for 1977 dollars) to compute the costs of the balance of the plant. The second model uses the cost model developed for tokamak system studies,[12] with proper adjustments. Both models predict capital costs of approximately $800-1200/KW(e). These relatively low costs reflect the simplicity of the EBTR design. In particular, the modular nature of individual blanket shield segments, the low-cost "accelerator style" containment building, high-β, and steady-state operation lead to relatively low reactor costs. The impacts of technology, engineering design, and plasma operating characteristics on the EBT plant cost are examined. A detailed cost breakdown for subsystems is analyzed and the results are discussed in Ref. 13.

Acknowledgement

The authors gratefully acknowledge the many helpful discussions with R. A. Dandl, R. A. Dory, and D. G. McAlees.

References

1. R. A. Dandl et al., "Research Program for Plasma Confinement and Heating in ELMO Bumpy Torus Devices," ORNL/TM-4941, Oak Ridge National Laboratory (June 1975); "The ELMO Bumpy Torus Program," ORNL/TM-5451, Oak Ridge National Laboratory (April 1976).
2. D. G. McAlees et al., "The ELMO Bumpy Torus Reactor (EBTR) Reference Design," ORNL/TM-5669, Oak Ridge National Laboratory (November 1976).
3. N. A. Uckan et al., "The ELMO Bumpy Torus (EBT) Reactor," ORNL/TM-6084, Oak Ridge National Laboratory (to be published).
4. D. B. Nelson, C. L. Hedrick, "Macroscopic Stability and Beta Limits in the ELMO Bumpy Torus," ORNL/TM-5567, Oak Ridge National Laboratory (to be published).
5. N. A. Uckan, C. L. Hedrick, "Plasma Simulation and Modeling for ELMO Bumpy Torus Reactor," ORNL/TM-6019, Oak Ridge National Laboratory (October 1977).
6. J. F. Clarke, "High Beta Flux-Conserving Tokamaks," ORNL/TM-5429, Oak Ridge National Laboratory (June 1976).
7. C. L. Hedrick et al., "A Simple Neoclassical Point Model for Transport and Scaling in EBT," ORNL/TM-5490, Oak Ridge National Laboratory (April 1977).
8. L. M. Kovrizhnykh, Sov. Phys.-JETP 29, 475 (1969).
9. J. N. Luton, H. T. Yeh, "Toroidal Magnet System Design for the ELMO Bumpy Torus Reactor," in Proc. 6th Int. Conf. on Magnet Technology (to be published).
10. W. W. Engle, Jr., "A User's Manual for ANISN, a One-Dimensional Discrete Ordinates Code with Anisotropic Scattering," Report K-1693, Computing Technology Center, Union Carbide Corporation (1967).
11. W. E. Ford et al., "Modification Number One to the Coupled 100n-21γ Cross-Section Library for EPR Calculations," ORNL/TM-5249, Oak Ridge National Laboratory (1976).
12. D. Steiner et al., "ORNL Fusion Power Demonstration Study: Interim Report," ORNL/TM-5813, Oak Ridge National Laboratory (March 1977).
13. J. T. Woo, N. A. Uckan, L. M. Lidsky, "Economic Analysis of EBT Reactor," paper presented at this conference.